Received: 8 May 2018 | Revised: 13 August 2018 | Accepted: 15 August 2018

DOI: 10.1111/pce.13435

ORIGINAL ARTICLE

WILEY Plant, Cell & Environment

Water relations determine short time leaf growth patterns in the mangrove *Avicennia marina* (Forssk.) Vierh.

Jonas Hilty | Chris Pook | Sebastian Leuzinger

Institute for Applied Ecology New Zealand, School of Science, Auckland University of Technology, Auckland, New Zealand

Correspondence
Jonas Hilty, Institute for Applied Ecology New Zealand, School of Science, Auckland University of Technology, 46 Wakefield Street, 1142 Auckland, New Zealand.
Email: jhilty@aut.ac.nz

Abstract

High-resolution leaf growth is rarely studied despite its importance as a metric for plant performance and resource use efficiency. This is in part due to methodological challenges. Here, we present a method for in situ leaf growth measurements in a natural environment. We measured instantaneous leaf growth on a mature *Avicennia marina* subsp. *australasica* tree over several weeks. We measured leaf expansion by taking time-lapse images and analysing them using marker tracking software. A custom-made instrument was designed to enable long-term field studies. We detected a distinct diel growth pattern with leaf area shrinkage in the morning and leaf expansion in the afternoon and at night. On average, the observed daily shrinkage was 37% of the net growth. Most of the net growth occurred at night. Diel leaf area shrinkage and recovery continued after growth cessation. The amount of daily growth was negatively correlated with shrinkage, and instantaneous leaf growth and shrinkage were correlated with changes in leaf turgor. We conclude that, at least in this tree species, instantaneous leaf growth patterns are very strongly linked to, and most likely driven by, leaf water relations, suggesting decoupling of short-term growth patterns from carbon assimilation.

KEYWORDS

auxanometer, *Avicennia marina*, diel growth cycle, instantaneous leaf growth measurement, leaf expansion, leaf shrinkage, mangrove, water relations

1 | INTRODUCTION

Plant growth is the single most important process to sustain life on earth. The net accumulation of phytomass can be quantified via a number of direct (dendrochronology, stem radius variation, biomass harvest, root ingrowth cores) or indirect (eddy covariance, remote sensing) methods. Most of these methods, however, integrate growth over long time spans and do not allow to quantify exactly when growth occurs during the day or night. Also, particularly modelling studies continue to use photosynthesis as a driver of plant growth (e.g., Mercado et al., 2018), despite evidence showing that in natural environments, other factors such as temperature, water, or nutrient availability directly limit growth long before photosynthesis is affected (Fatichi, Leuzinger, & Körner, 2014). The abundance of photosynthesis data and their misinterpretation as a proxy for growth exists at least partly because measurements of leaf gas exchange have become relatively straightforward, with easy-to-use and portable instruments. In contrast, nondestructive measurements of high-resolution leaf and plant growth are technically much more challenging, particularly in the field. Nevertheless, measuring instantaneous leaf growth is pivotal for understanding the influence of environmental and endogenous drivers on plant resource efficiency and performance (Walter, Silk, & Schurr, 2009). A fundamental understanding of the mechanisms of plant growth will also inform a new generation of carbon sink-driven ecosystem models (Leuzinger, Manusch, Bugmann, & Wolf, 2013).

Leaf growth is approximated by observing leaf area over time. The development of leaf area is the result of three main processes: cell proliferation, expansive cell growth, and elastic cell swelling and shrinkage. It is not possible to clearly distinguish between the three

processes from nondestructive measurements, especially in dicotyledons where all processes can occur simultaneously in the same region of the leaf. Therefore, net leaf area change is often equated with growth, which ignores elastic deformation. In this paper, we adopt the terminology from the analysis of stem radius variations, which has long dealt with similar analytical challenges, and that postulates that growth is negligible in periods of shrinkage (Zweifel, Haeni, Buchmann, & Eugster, 2016). Periods of elastic shrinkage and swelling are called water deficit periods and are distinguished from periods with irreversible growth.

Traditional auxanometers that automatically measure plant or leaf elongation rely on the application of a tensile force to keep the object stretched, and they record changes in the position of the tip (Hsiao, Acevedo, & Henderson, 1970; Pfeffer, 1903). A similar principle has also been used to measure leaf elongation of grasses in the field (Nagelmüller, Kirchgessner, Yates, Hiltpold, & Walter, 2016). In recent years, new methods emerged that use digital image analysis to quantify plant characteristics (Minervini, Scharr, & Tsaftaris, 2015). However, many of these methods are designed for indoor use and do not focus on high-resolution growth measurements. Outdoor conditions are particularly challenging because direct sunlight can interfere with the sensor measurement, and electronic components require protection from rain, humidity, and overheating. A relatively simple method to measure leaf area growth of dicotyledons is to fix a leaf in a plane and observe it through a camera with the image plane parallel to the leaf (Schmundt, Stitt, Jahne, & Schurr, 1998; Walter, Feil, & Schurr, 2002). Relying on this principle, Mielewczik, Friedli, Kirchgessner, and Walter (2013) presented a semiautomated image analysis software based on marker tracking, and they also showed the general feasibility of their method for field studies.

For dicotyledons, two different instantaneous leaf growth types have been described. One growth form shows the highest growth rates around dawn and the lowest rates around dusk, whereas the other form shows a reversed pattern with growth peaking around dusk (Walter et al., 2009). In contrast, leaf elongation in monocots largely follows meristem temperature, and the highest growth rates occur at midday (Walter et al., 2009). However, in *Zea mays*, leaf elongation rates during daytime are lowered by evaporative demand when expressed in thermal time (Sadok et al., 2007). Dicotyledons show a diel leaf growth cycle that is partly controlled by the circadian clock (Poire et al., 2010; Ruts, Matsubara, Wiese-Klinkenberg, & Walter, 2012). A circadian regulation is thought to optimize resource use throughout the day and to buffer against short-term environmental fluctuations that are especially pronounced for dicot leaves (Walter et al., 2009). For example, growth does not respond to short-term temperature changes (Poire et al., 2010), and the circadian clock seems to be involved in the overnight partitioning of starch (Apelt et al., 2017). Young *Arabidopsis thaliana* leaves have lowered growth rates at night, which is associated with carbon metabolism. After a few days, this shifts to lower growth rates during daytime, when leaf expansion is limited by hydraulics (Pantin, Simonneau, & Muller, 2012; Pantin, Simonneau, Rolland, Dauzat, & Muller, 2011).

Here, we present the first data on in situ leaf growth of a mature tree. We measured instantaneous leaf growth on an *Avicennia marina* subsp. *australasica* tree over several weeks using the leaf fixation method. *Avicennia marina* is highly salt tolerant and is therefore an interesting model species to study the interplay between environmental conditions, water relations, and growth processes (Ball, 1988). Our study site also has the advantage of a monospecific stand, where even mature tree crowns are easily accessible, avoiding confounding of succession and interspecific competition. Our aims were (a) to test the usability of instantaneous leaf growth measurements in situ in adult trees, (b) to identify when exactly leaves grow during the day or night at a subhourly resolution, and (c) what environmental or plant-intrinsic parameters drive this growth.

2 | MATERIALS AND METHODS

2.1 | Instrument design

We modified the method described by Mielewczik et al. (2013) for long-term outdoors use. The basic principle of this method is to fix the leaf in a frame to limit horizontal movement and prevent vertical movement (Figure 1a). A camera was mounted with the image plane parallel to the leaf, and image time series were acquired. Leaf expansion was approximated by tracking artificial markers placed at the leaf fixation points. The development of the area spanned between the markers served as a proxy for relative leaf area change.

For the application of this method in the field, we designed a compact and weatherproof instrument, which is easy to install and allows reliable data acquisition. Pictures were taken using a Pi NoIR v2 camera controlled by a Raspberry Pi 1 B+ single board computer (Raspberry Pi Foundation, Cambridge, UK). The Pi NoiR v2 does not have an infrared filter, which makes night vision possible. To continuously measure leaf growth at night, we used two infrared light-emitting diodes (LEDs) with a peak wavelength of 850 nm, which were attached to the Pi NoIR camera (Shenzhen Xingmu Technology Co., Ltd, Shenzhen, China; purchased on alibaba.com).

Pictures were taken every 5 min and uploaded to a server. This allowed for continuous monitoring of the experiment and also served as a backup. The picture resolution was 1,296 × 972 pixels; JPEG compression was applied to reduce the file size. The infrared LEDs were switched on 5 s before taking a picture and switched off afterwards to minimize any potential effect on physiological processes. This was controlled using an Arduino Nano board (Arduino SA, Chiasso, Switzerland) connecting the Raspberry Pi with a relay in the LED's power supply. A detailed sketch of the technical components is given in Figure S1. All processes were executed in a Python script (Version 3.5, Python Software Foundation, Wilmington, DE) running on the Raspberry Pi.

The instrument design included a frame where the leaf was fixed, a housing parallel to that frame containing the camera and LEDs, a separate housing for the Raspberry Pi and other components, and a third external housing containing a Huawei E5330 mobile 3G router (Huawei Technologies Co. Ltd, Shenzhen, China), and a power converter. The camera was placed 25 cm above the leaf frame. Individual elements were laser cut from 6 mm thick acrylic and glued together. During the experiment, the instrument was covered with an aluminium hood for additional rain and radiation protection.

FIGURE 1 Experimental set-up. (a) Sample image at the start of the experiment. The leaf is fixed in a plane using small wooden pegs. Markers for the image analysis are placed on the pegs. Six light sensors are placed on the frame around the leaf. (b) Temperature and relative humidity sensor just below the leaf growth meter. (c) Assembled instrument

The instrument was fixed with T-head bolts on a matching frame built with aluminium strut profiles (Bosch Rexroth AG, Lohr am Main, Germany), which was strapped to a horizontal pole. The leaf was fixed and kept flat using five small wooden pegs connected to small lead weights of 7 g each. The surfaces of the pegs were coloured black using a waterproof pen with one spot left blank to serve as the marker for the image analysis (Figure 1a). The application of tensile forces to the leaf could potentially cause changes in growth behaviour. In a control experiment, we show that the treatment did not affect long-term leaf growth in *A. marina* (Figure S2). In general, the forces need to be high enough to keep the leaf in place in windy conditions but low enough to not affect growth. *A. marina* has quite sclerophyllous leaves, and the leaf was not damaged by the pegs or the tensile force. However, after the experiment, the fixation points were clearly visible by a lack of chlorophyll on the adaxial surface and slightly visible on the abaxial surface (Figure S3). Additionally, Leaf 1 seemed to have a slight growth reduction at the fixation points at the leaf side (Figure S3a). A general limitation of this method is that it cannot be used for young leaves that are too small or too fragile for fixation. Further, the fixation of leaves can alter growth patterns in species with leaf hyponasty, even when low tensile forces are applied (Walter et al., 2002). We therefore analysed leaf angle variations from unrestricted leaves visible within our picture frames, but although they changed randomly with wind throughout the day, there was no diurnal trend.

2.2 | Experiment

The measurements were conducted on a mature tree of the mangrove *A. marina* (Forssk.) Vierh. subsp. *australasica*. The research site was located in the Mangawhai Heads estuary at the east coast of New Zealand's North Island (36.097°S, 174.573°E). In this environment, *A. marina* grows in uniform, monospecific forests with trees reaching mean heights of 3.1 m (Tran, Gritcan, Cusens, Alfaro, & Leuzinger, 2017). The forest covers an area of approximately 0.8 km^2 located around Tara Creek. Power was available from a small photovoltaic system.

The experiment was conducted on two different leaves on the same tree: the first from mid December 2016 to early January 2017 and the second from early February to early March 2017. Young leaves at the top of the canopy facing north were selected for the experiment to minimize shading from the instrument. Additionally, for the second run, a relatively large leaf was chosen in order to observe growth cessation. To restrict movements of the leaf, the branch on which it was growing was fixed to the strut frame using Velcro straps (Velcro Ltd, Middlewich, UK). The leaf opposite to the observed one was bent backwards because it would otherwise have obstructed the view of the markers (Figure 1a). In December, we also installed two leaf turgor pressure probes in the same tree (YARA ZIM Plant Technology GmbH, Hennigsdorf, Germany). Those sensors measure a magnetic force between two clamps that are inversely proportional to leaf turgor (Zimmermann et al., 2008). It can only be interpreted as a relative signal of turgor change, because the measured pressure depends on the cell elastic modulus, which can vary with temperature.

Environmental data were measured close to the leaf as well as above canopy on a tower approximately 5 m away from the experiment. Leaf illuminance was measured in intervals of 1 min using six HOBO UA-002-64 data logger (Onset Computer Corporation, Bourne, MA; spectral range 150 to 1,200 nm) that were placed around the leaf (Figure 1a). Local air temperature and relative humidity were measured in intervals of 5 min using a HOBO Pro v2 U23-002 data logger (Onset Computer Corporation, Bourne, MA) located below the instrument (Figure 1b). The saturation water pressure was calculated according to Buck (1981), and the vapour-pressure deficit (VPD) was derived from it. Above canopy solar radiation was measured using a pyranometer (model PYR, Decagon Devices, Inc., Pullman, WA; spectral range 380 to 1,120 nm). Precipitation was measured using a tipping-bucket rain gauge (Model 52203, R. M. Young Company, Traverse City, MI; resolution of 0.1 mm per tip). The precipitation

sensor broke between the first and second experimental run. For the second period, the time of precipitation was determined from inspecting the recorded images, and the intensity was estimated using measurements from the Mangawhai Heads Weather Station, located approximately 2 km from the research site. Tidal flooding was reconstructed from previous measurements (Donnellan Barraclough, Zweifel, Cusens, & Leuzinger, 2018), and water depth measurements in Auckland (36.833°S, 174.783°E) obtained from Land Information New Zealand (2017).

We also conducted a seasonal leaf growth experiment from May 2017 until February 2018 to test for seasonal leaf growth variations. The experiment took place at Panmure Basin, Auckland (36.907°S, 174.845°E). We started cohorts in fall (May 2017), winter (July 2017), and summer (December 2017 and January 2018). For each cohort, we selected 10 young leaves on five different trees (two leaves per tree). Leaf length and maximal width were measured every few weeks with callipers.

2.3 | Data analysis

Relative leaf area change was measured using a custom-made marker tracking software similar to *Martrack Leaf* (Mielewczik et al., 2013). We did not use Martrack Leaf because it turned out to be sensitive to movements due to wind. However, in nonwindy conditions, our software and Martrack Leaf show similar results (Figure S4). We also conducted a control run with a carbon fibre plate instead of a leaf. We did not observe any systematic diel trends, and the measurement error was approximately 0.5% (not shown).

Our marker tracking software is semiautomated; in case of misdetections, the user needs to redefine the marker location. This happened in windy conditions when the leaf was moved more than the software's maximal search range set at an upper limit of approximately 2.8 mm. The software is a console application written in C++ (Standard C++ Foundation, Redmond, WA) using the open-source image analysis library OpenCV (Bradski & Kaehler, 2008).

The detected marker locations can be noisy due to slight movements of the leaf caused by wind, or due to changes in illumination. Therefore, the measured relative leaf area was adjusted by outlier removal and subsequent smoothing. We applied the *loess* smoothing (Cleveland, 1979; Cleveland & Devlin, 1988) with second-degree polynomial regression, weighted least squares fitting, and a neighbourhood of 49 data points, which translates to a smoothing window of approximately 4 hr. The leaf turgor data were smoothed using the same parameters.

Statistical analysis was conducted using R Version 3.4.2 (R Core Team, 2017); environmental data were matched to the nearest leaf area measurement. Instantaneous relative area change (RAC) was calculated for every measurement from the smoothed values:

$$RAC_i = \frac{A_i - A_{i-1}}{A_{i-1}} \cdot 100,$$

where A_i represents the area for measurement i. The relative growth rate (RGR) was calculated on the basis of the exponential growth formula (Blackman, 1919):

$$RGR_i = \frac{\ln\left(\frac{A_i}{A_{i-1}}\right)}{t_i - t_{i-1}} \cdot 100,$$

where t_i represents a point in time, and the time difference between two measurements is expressed in hours. For periods of leaf shrinkage, we calculated the relative *leaf water deficit* (LWD) compared to the previous maximum area:

$$LWD_i = \frac{\max(A_{j \le i}) - A_i}{\max(A_{j \le i})} \cdot 100.$$

The LWD is similar to the concept of *tree water deficit* used to describe stem shrinkage (Zweifel et al., 2016). A distinction between a water deficit and a growth phase rather than between a shrinkage and an expansion phase assumes that structural growth is largely absent in water deficit periods. During LWD periods, RGR does not actually measure growth but rather elastic leaf area changes. Normalized leaf turgor change (TG) was calculated like the following:

$$D_i = \left(\frac{1}{P_i} - \frac{1}{P_{i-1}}\right), \quad TG_i = D_i \cdot \frac{1}{\max(|\min(\mathbf{D})|, |\max(\mathbf{D})|)}$$

where P_i represents the clamp pressure at time i and $\mathbf{D}$ represents a vector of all observed turgor changes D_i. Leaf growth and environmental data are shown in Figure 2. The absolute leaf area was estimated from a regression model based on pixel counting (Figure S5), with the pixel size known from the camera geometry and object distance.

3 | RESULTS

We measured instantaneous leaf area change on a mature tree in its natural environment over several weeks. Our measurements show a distinct diel leaf growth cycle that starts in the morning after dawn when the leaf area reaches a local maximum. Subsequently, the leaf is shrinking until a local minimum is reached around noon, after which it is expanding again in the afternoon and during the night (Figures 2a,b, 3). The mean daily net growth was 2.9% (standard deviation [*SD*] = 2.1%), and the mean maximum shrinkage was 1.1% (*SD* = 1.0%) when aggregated by time since the last peak (Figure 3). On average, leaf shrinkage was 37% of the daily net growth. The re-expansion to the previous maximum took place until late afternoon, which means that most of the net growth occurred at night. In general, a small shrinkage was followed by a larger net growth (Figure 4c). Relative leaf area change was strongly correlated with changes in leaf turgor (Figure 4a,b).

Leaf 1 was observed over a period of 16 diel cycles from December 17, 2016, to January 2, 2017 (Figure 2a). During the experiment, it expanded from a minimum of approximately 472 mm^2 in the night after the installation to 1,340 mm^2 at the end of the measurement, which is an increase by 183.8%. The second leaf was observed over 29 diel cycles and only showed a small area increase of 15.2% from approximately 824 mm to 950 mm^2 (Figure 2b). The growth mainly occurred in the first 7 days after the start of the measurement from February 3 to 10, 2017, referred to as Leaf 2A. This was followed by Phase 2B, a 9-day period of strong leaf shrinkages and gradual recovery, ending on February 19, 2017, after 2 days of little

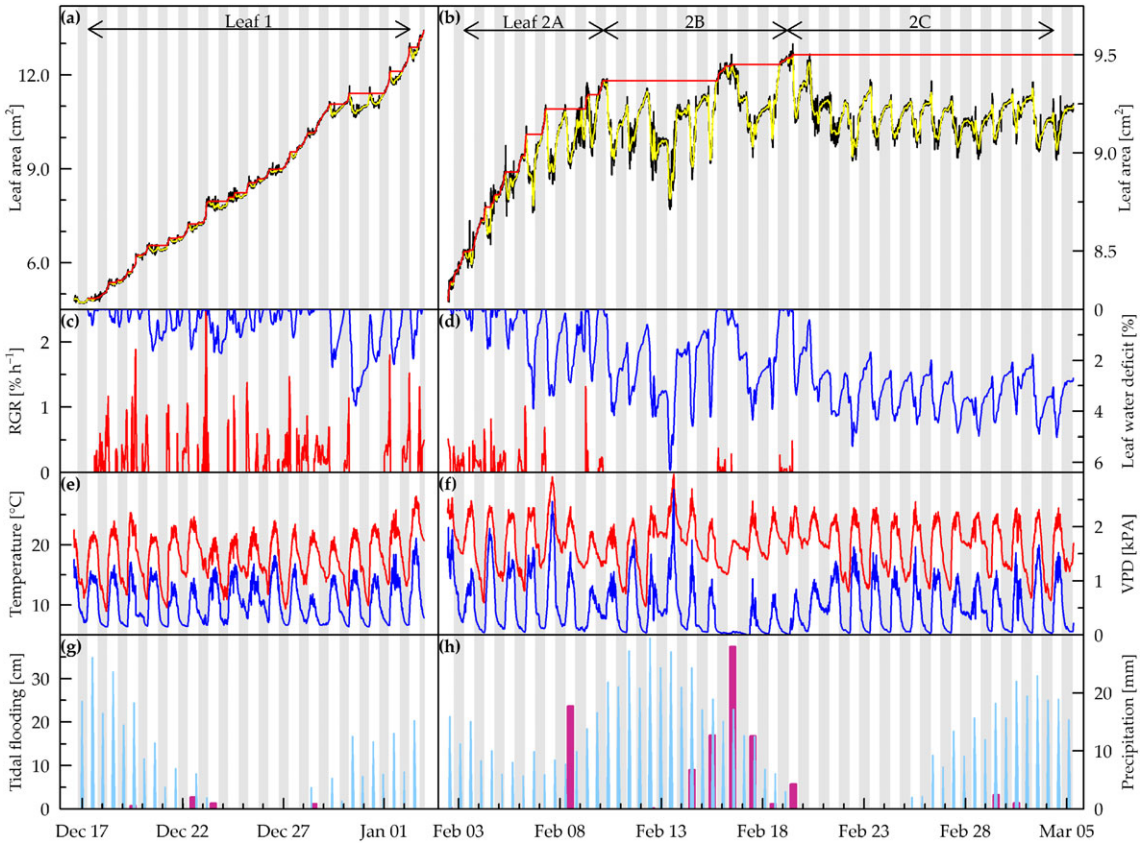

FIGURE 2 Leaf area change and environmental variables. (a, b) Absolute leaf area development: raw data in black, smoothed curve in yellow, and cumulative maximum based on smoothed curve in red. The arrows indicate different growth phases (see text). (c, d) Relative growth rate (RGR) from frame to frame in red (only shown for growth periods) and leaf water deficit in blue. (e, f) Local air temperature in red and vapour-pressure deficit (VPD) in blue. (g, h) Water depth during tidal flooding in light blue and precipitation sum per diel cycle in purple. Shaded areas represent night as measured by the illuminance sensors next to the leaf

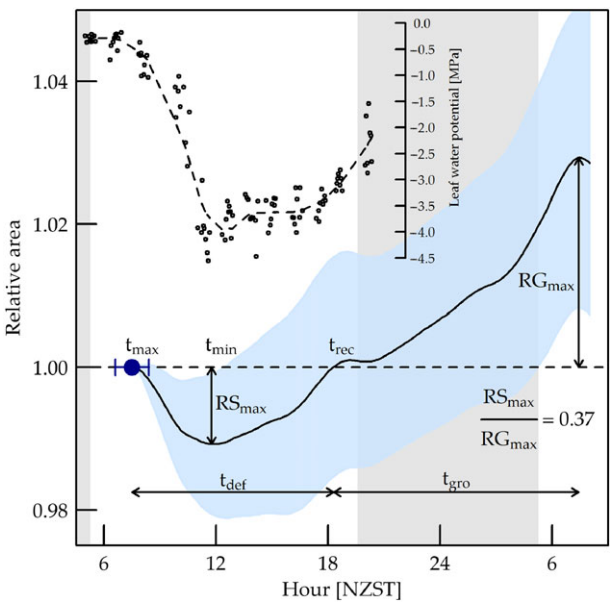

FIGURE 3 Mean relative diel growth cycle from one local maximum to the next for Leaves 1 and 2A (n = 23). One standard deviation of the area is shaded in blue. The standard deviation of t_{max} is given by the dark blue error bar. The x-axis shows time since t_{max} but converted to 24-hr clock time for better readability. The inset shows leaf water potential measurements from February 13, 2015 (Donnellan Barraclough et al., 2018). NZST, New Zealand Standard Time

net growth. During the last 13 days of the measurement until March 4, 2017, Phase 2C, the leaf did not grow any further but continued a diel cycle of area shrinkage and expansion. We hypothesize that the early growth cessation of Leaf 2 might reflect a seasonal effect. The seasonal leaf growth experiment confirmed leaf growth variations throughout the year. Leaves that emerged in December 2017 or January 2018 were growing at higher rates and to larger sizes than were leaves that emerged in May 2017, whereas leaves that emerged in July 2017 were growing at lower rates and remained smaller (Figure S6).

Figure 3 shows the mean diel growth cycle from Leaf 1 and Leaf 2A (n = 23) aggregated by time after the local area maximum, and defines key metrics for our analysis. We divided the diel growth cycle into two phases: a water deficit phase during which the leaf area is below the previously measured maximum in the early morning and a growth phase, exceeding the previous maximum. The deficit phase can be further divided into a shrinkage phase and a recovery phase. The shrinkage phase starts at the time of the local area maximum in the morning (t_{max}) and ends when the area reaches a minimum (t_{min}). During the recovery phase, the leaf expands again to the previous area maximum, which is reached at t_{rec}. The relative net growth RG_{max} in one diel cycle is the leaf area at the end relative to the start. It cannot be quantified which part of RG_{max} is the result of growth processes and which part results from elastic swelling. The relative maximal shrinkage RS_{max} is the minimal leaf area during a diel cycle relative to the initial leaf area. Our analysis also includes two diel cycles with

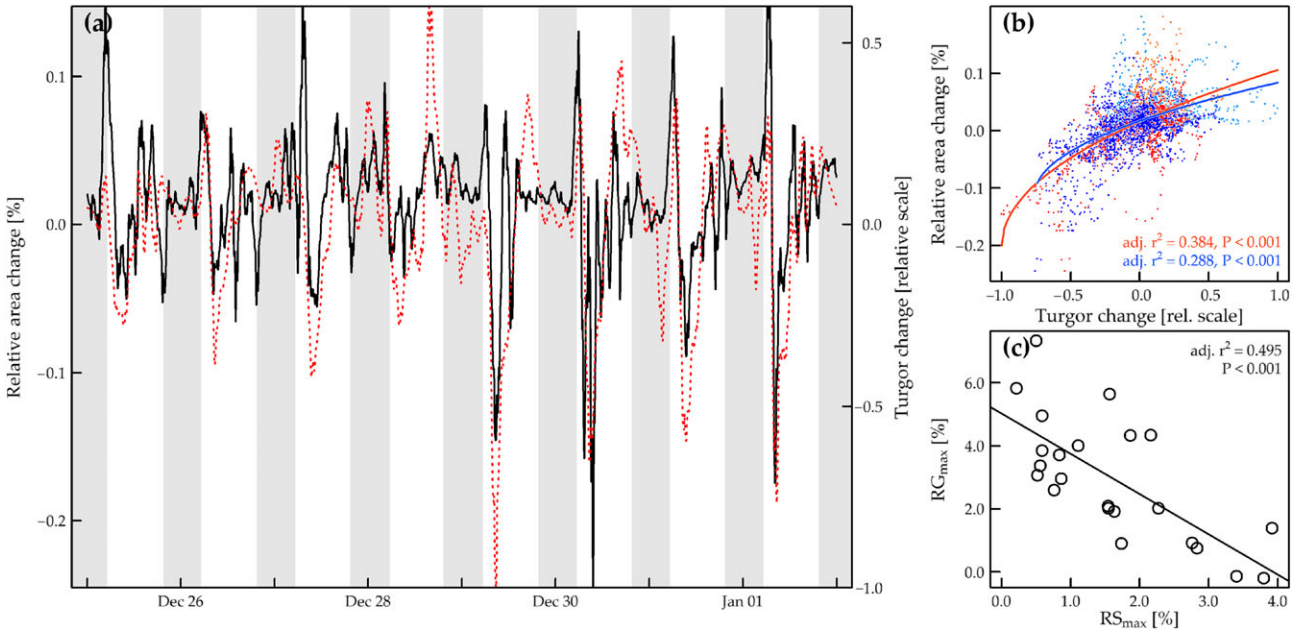

FIGURE 4 Correlation of leaf water status with leaf area changes. (a) Time series of relative area change (black) and turgor change of a different leaf on the same tree (dotted red) from December 25, 2016, to January 1, 2017. (b) Regression curve for the same sensor in light red; red points represent observations during leaf water deficit, orange points during growth phases, and the same for a second turgor sensor that preceded leaf growth by ~55 min in blue; dark blue points represent observations during leaf water deficit, and light blue points during growth phases. Linear models were fit after shifting the data to non-negative values, and square root transformation. (c) Linear regression between maximum diel growth (RG_{max}) and shrinkage (RS_{max}) for Leaves 1 and 2A combined

slightly negative RG_{max} (effectively a net shrinkage): from December 30 to 31, 2016, with a net area decrease of 0.18%, and from February 7 to 8, 2017, with a decrease of 0.13%.

The leaf shrinkage started at 7:21 a.m. New Zealand Standard Time (*SD* = 53 min), or 119 min after dawn (*SD* = 59 min). Dawn was defined as a leaf illuminance of more than 425 lux. The diel growth cycles for each leaf individually are shown in Figure S7a. The two observed leaves started shrinking at the same hour of the day. However, Leaf 1 had a lower RS_{max} and a higher RG_{max} than had Leaf 2A. The aggregated t_{min} for Leaves 1 and 2A combined was at 11:45 a.m. New Zealand Standard Time; there was no significant difference between the two leaves. In Phases 2B and 2C, the timing of the diel cycle was not as distinct as in Leaves 1 and 2A. The shrinkage started usually around dawn as well, but sometimes earlier. Additionally, t_{min} was only reached in the early afternoon (Figure S7b).

Table 1 shows linear correlations between environmental variables aggregated over the night-time and daytime, respectively, and the extent of RS_{max}, RG_{max}, as well as t_{max}, and the duration of the deficit phase, t_{def}. The mean night temperature preceding the observed diel cycle marginally correlated with RS_{max}, RG_{max}, and t_{def}. The warmer the previous night, the higher was the relative shrinkage, the longer the LWD period, and the smaller the relative growth. However, none of these measures correlated with the mean VPD of the previous night. For the mean day temperature, we observed a marginally significant correlation with RS_{max}, but no correlation with any other variables. For the mean daytime VPD, on the other hand, we observed a marginally significant positive correlation with RS_{max} and a significant negative correlation with RG_{max}. The mean radiation was also significantly negatively correlated with RG_{max}. Tidal flooding and precipitation are not included in Table 1, because we could not find any correlation between the time or height of the tide and leaf growth parameters, and there were too few rain events in our dataset for a quantitative analysis. For the daily cycle, we observed a strong negative correlation between RS_{max} and RG_{max} (Figure 4c).

TABLE 1 Correlations between key metrics defined in Figure 3 and average environmental conditions (temperature, *T*; vapour-pressure deficit, *VPD*; and radiation, *E*) in the night previous to the cycle (np) and during the day (d)

	$\overline{T_{np}}$	$\overline{VPD_{np}}$	$\overline{T_d}$	$\overline{VPD_d}$	$\overline{E_d}$
RS_{max}	↗• 0.087	ns	↗• 0.098	↗• 0.085	ns
RG_{max}	↘• 0.117	ns	ns	↘** 0.245	↘* 0.177
t_{def}	↗• 0.089	ns	ns	ns	↗• 0.123
t_{max}	ns	ns	n/a	n/a	n/a

Note. The → indicate the direction of the correlation; significance of *P* values is indicated as follows: •, 0.10 > *P*; *, 0.05 > *P*; **, 0.01 > *P*. Adjusted r^2 values are given below. t_{max} was expressed in decimal hour of day.

The in situ relative leaf area change and change of leaf turgor followed a similar diel pattern and were strongly correlated in a non-linear way (Figure 4a,b). Both turgor sensors showed a similar trend (not shown), but with a time lag of 55 min between the two observed leaves, which was corrected before the correlation analysis. Linear models were fit after shifting the turgor change data to non-negative values, and square root transformation:

$$RAC_i = a \cdot \sqrt{|\min(\boldsymbol{TG})| + TG_i} + b + \epsilon.$$

During LWD periods, turgor had a stronger impact on relative area changes (shrinkage and re-expansion) than during growth periods (Figure 4b).

We also tested for correlations between in situ RGR and environmental variables. We did not find any pattern other than small but highly significant negative correlations with temperature, VPD, and irradiance, which reflect the opposite diel cycles of leaf area and temperature, VPD, and irradiance, respectively. Scatterplots of environmental variables and RGR for different growth phases are shown in Figure S8.

4 | DISCUSSION

This paper reports the development of a bespoke, inexpensive, and open-source instrument for long-term measurement of instantaneous leaf area changes in the field. We observed a clear diel growth pattern with considerable leaf area shrinkage in the morning and leaf expansion in the afternoon and at night. On average, the shrinkage was 37% of the diel net growth, which, to our knowledge, is the highest value ever observed over a prolonged growth period. Diel leaf growth was limited by the amount of leaf shrinkage immediately preceding growth, and relative leaf area changes were strongly correlated with leaf turgor changes. Together, these correlations strongly suggest that in *A. marina* instantaneous leaf growth patterns are driven by leaf water relations, and not by carbon assimilation. This supports the view that leaf growth is generally limited by hydraulics (Pantin et al., 2012).

Leaf expansion can directly be limited by water stress; for example, leaf elongation in *Z. mays* shows an immediate response to changes in soil water potential (Hsiao et al., 1970), or evaporative demand (Bouchabké, Tardieu, & Simonneau, 2006). In *Helianthus annuus*, a soil water deficit leads to a decrease in long-term relative leaf growth rates, resulting from a reduction in cell number, or cell size, depending on leaf ontogeny (Granier & Tardieu, 1999). In general, soil water deficits have a much stronger negative effect on shoot growth than on photosynthesis (Muller et al., 2011). Our results strongly support these findings.

Avicennia marina has a high salinity tolerance, and long-term leaf area expansion rates decrease with increasing salinity (Ball, 1988). Here, we showed that water stress led not only to an in situ growth reduction but to a pronounced period of leaf area shrinkage. Leaf shrinkage in growing leaves has been described before in *Tripolium pannonicum* (*Aster tripolium*) and *Beta vulgaris* exposed to salt water (Rozema, Arp, Diggelen, Kok, & Letschert, 1987; Waldron, Terry, & Nemson, 1985). Short periods of leaf area decrease of up to 2 hr have also been observed in *Glycine max* (Mielewczik et al., 2013) and *A. thaliana* (Apelt et al., 2017).

Our observations suggest that the extent of the diurnal leaf shrinkage limits diel growth (Figure 4c). The decrease in leaf area seems to be driven by water loss through transpiration, concurrent with a strong drop in leaf water potential (Figure 3), and a decrease in leaf turgor (Figure 4a,b). Despite a lower leaf water potential in the late afternoon compared with midmorning, we observed shrinkage in the morning and leaf expansion in the late afternoon (Figure 3). This is a classic hysteresis response and can only be due to changes in osmolyte concentrations, or plant-intrinsic hydraulic properties (elastic modulus, xylem conductivity, cell wall extensibility). The correlation between leaf turgor and area change was non-linear, suggesting that turgor had a stronger impact on elastic deformation during water deficit periods than on growth.

It has recently been reported that extracellular water storage and water uptake from the air by trichomes contribute to the maintenance of leaf water status of *A. marina* (Nguyen, Meir, Wolfe, Mencuccini, & Ball, 2017). We often observed an RGR peak in the early morning (Figure 2c,d), and it could be speculated that this reflects direct leaf water uptake from dew or air of high relative humidity surrounding the leaf, and not structural growth. Earlier measurements of water relations of the same species and at the same site support this: The highest stomatal conductance values were observed in the morning, after which they declined (Donnellan Barraclough et al., 2018). Leaf water potential measurements on February 13, 2015, ranged from a predawn maximum of −0.6 MPa to a minimum of −4.1 MPa in the early afternoon (Donnellan Barraclough et al., 2018). Pressure–volume curves of the same species growing in Australia showed that a decrease in water potential below −0.9 MPa is driven by a decline in turgor (Nguyen, Meir, Sack, et al., 2017). Our observed midday leaf water potentials are close to the turgor loss point, which depends on salinity and occurs between −4.5 and −5.1 MPa in *A. marina* subsp. *australasica* (Nguyen, Meir, Sack, et al., 2017). In this domain, the relative leaf water content decreases from approximately 87% to 76%, which translates to a decrease in leaf volume of about 13%. This potential volume loss results from a modulus of elasticity of about 26 MPa (Nguyen, Meir, Sack, et al., 2017). The highest leaf area shrinkage we observed in our experiment was 6.4% on February 13, 2017. If we assume that leaf thickness decreased by a similar amount, the total volume loss would be close to the total water storage before turgor loss. Therefore, we conclude that the observed leaf area shrinkage was driven by water loss, similar to the observed decline in turgor (Figure 4a,b), and leaf water potential (Figure 3).

We did not investigate whether the observed growth was driven by cell proliferation, or expansion, or both. On the basis of the approximately linear long-term growth (Figure 2a,b), we assume that turgor-driven cell expansion was the dominant process, but this may well be different for emerging leaves, where ontogenetic growth regulation is important (Pantin et al., 2011). Some limited growth activities may still be present during water deficit periods, as it has been observed for stem shrinkage (Zweifel et al., 2016). Such "stored growth" leads to higher initial growth rates after the deficit period. However, we were unable to detect this effect in the present study.

Our marker tracking software performed well in all but the windiest conditions. We obtained a slightly noisy relative leaf area signal that required smoothing for further analysis (Figure 2a,b). The choice of smoothing parameters does affect the observed in situ RGR, as well as the exact t_{max}, t_{min}, and t_{rec}. However, the general observation of a diel growth cycle is unaffected, and the extent of the relative shrinkage RS_{max} and relative growth RG_{max} are largely independent of the smoothing parameters. Applying the same analysis to the control data obtained with a carbon fibre plate showed that there was no artifactual diel trend (Figure S9). The method could be further improved by a better marker design that would allow for a less noisy tracking, for example, by using the ArUco library (Garrido-Jurado, Muñoz-Salinas, Madrid-Cuevas, & Marín-Jiménez, 2014).

We found marginally significant correlations between the mean temperature of the previous night and RS_{max}, and RG_{max}, respectively (Table 1). We cannot think of any hydraulic process that could explain this correlation, especially because night VPD did not correlate with any of the measured parameters. However, it could be speculated that higher night temperatures lead to a depletion of carbohydrate reserves, which reduces the ability to maintain turgor in the morning. A mechanistic explanation would need a set of dedicated additional measurements such as high-resolution leaf osmotic potential, and leaf starch and sugar content. On the other hand, mean daytime VPD correlated marginally positively with RS_{max} and negatively with RG_{max}. It can be expected that a higher VPD increases leaf water stress and thus LWD and so indirectly decreases the potential for growth (Figure 4c). The observed negative correlation between mean radiation and RG_{max} might reflect an indirect effect, because radiation and VPD were highly correlated (not shown).

Our study demonstrates the importance of high-resolution leaf growth measurements to detect and characterize minute changes in leaf area. In an experiment with only one or two measurements per day, for example, by using a smartphone app such as Petiole (petioleapp.com), the diurnal shrinkage could have remained undetected, and the dependence of leaf growth on water relations in *A. marina* would have been much harder to establish. By measuring instantaneous leaf area changes, we showed a strong correlation with leaf turgor (Figure 4a,b). Leaf turgor seems to have a stronger influence on shrinkage and re-expansion than on structural growth (Figure 4b), and the extent of diel shrinkage limits diel growth (Figure 4c). The limitation of leaf growth by water relations has been shown before for agricultural crops or the model species *A. thaliana*, and the importance of turgor for cell expansion is reflected in the Lockhart model (Lockhart, 1965; Ortega, 1985). Here, we show that water limitations also directly limit instantaneous leaf growth of a mature tree, namely, the mangrove *A. marina*. Measurements of non-structural carbohydrates at our site (material in preparation) indicate that although carbon is important as an osmolyte (sugar), it is hardly limiting under natural conditions. We therefore argue that there is no carbon trade-off involved, and instantaneous growth patterns are largely driven by plant hydraulic relations in this species. This may simply be a consequence of life in saline conditions but, if confirmed for other species, may point at a subordinate role of carbon in comparison with water when plant growth, at least at the scale reported here, is concerned. This adds to the paradigm that plant growth processes are generally decoupled from carbon assimilation, as has been shown for larger spatiotemporal scales (Körner, 2003). High-resolution leaf growth data under realistic in situ conditions are understudied but urgently needed to inform plant hydraulic and growth models (e.g., Steppe, De Pauw, Lemeur, & Vanrolleghem, 2006), whose improvement in turn is pivotal for a better understanding of vegetation modelling in a future climate (Fatichi, Pappas, & Ivanov, 2016).

ACKNOWLEDGEMENTS

We thank Alicia Donnellan Barraclough and Jarrod Cusens for sharing the leaf water potential data used in Figure 3. We also acknowledge the preliminary work on this project that was carried out by Katrin Hoffmann.

ORCID

Jonas Hilty http://orcid.org/0000-0003-0748-5998
Chris Pook http://orcid.org/0000-0002-0932-1965
Sebastian Leuzinger http://orcid.org/0000-0001-9306-5281

REFERENCES

Apelt, F., Breuer, D., Olas, J. J., Annunziata, M. G., Flis, A., Nikoloski, Z., … Stitt, M. (2017). Circadian, carbon, and light control of expansion growth and leaf movement. *Plant Physiology*, *174*, 1949–1968.

Ball, M. C. (1988). Salinity tolerance in the mangroves *Aegiceras corniculatum* and *Avicennia marina*. I. Water use in relation to growth, carbon partitioning, and salt balance. *Functional Plant Biology*, *15*, 447–464.

Blackman, V. H. (1919). The compound interest law and plant growth. *Annals of Botany*, *33*, 353–360.

Bouchabké, O., Tardieu, F., & Simonneau, T. (2006). Leaf growth and turgor in growing cells of maize (*Zea mays* L.) respond to evaporative demand under moderate irrigation but not in water-saturated soil. *Plant, Cell & Environment*, *29*, 1138–1148.

Bradski, G., & Kaehler, A. (2008). *Learning OpenCV*. Sebastopol, CA: O'Reilly Media, Inc.

Buck, A. L. (1981). New equations for computing vapor pressure and enhancement factor. *Journal of Applied Meteorology*, *20*, 1527–1532.

Cleveland, W. S. (1979). Robust locally weighted regression and smoothing scatterplots. *Journal of the American Statistical Association*, *74*, 829–836.

Cleveland, W. S., & Devlin, S. J. (1988). Locally weighted regression: An approach to regression analysis by local fitting. *Journal of the American Statistical Association*, *83*, 596–610.

Donnellan Barraclough, A., Zweifel, R., Cusens, J., & Leuzinger, S. (2018). Daytime stem swelling and seasonal reversal in the peristaltic depletion of stored water along the stem of *Avicennia marina* (Forssk.) Vierh. *Tree Physiology*, *38*, 965–978.

Fatichi, S., Leuzinger, S., & Körner, C. (2014). Moving beyond photosynthesis: From carbon source to sink-driven vegetation modeling. *New Phytologist*, *201*, 1086–1095.

Fatichi, S., Pappas, C., & Ivanov, V. Y. (2016). Modeling plant–water interactions: An ecohydrological overview from the cell to the global scale. *Wiley Interdisciplinary Reviews: Water*, *3*, 327–368.

Garrido-Jurado, S., Muñoz-Salinas, R., Madrid-Cuevas, F. J., & Marín-Jiménez, M. J. (2014). Automatic generation and detection of highly reliable fiducial markers under occlusion. *Pattern Recognition*, *47*, 2280–2292.

Granier, C., & Tardieu, F. (1999). Water deficit and spatial pattern of leaf development. Variability in responses can be simulated using a simple model of leaf development. *Plant Physiology*, *119*, 609–619.

Hsiao, T. C., Acevedo, E., & Henderson, D. W. (1970). Maize leaf elongation: Continuous measurements and close dependence on plant water status. *Science*, *168*, 590–591.

Körner, C. (2003). Carbon limitation in trees. *Journal of Ecology*, *91*, 4–17.

Land Information New Zealand (2017) Sea level data downloads, Wellington, New Zealand. Web Page. Retrieved 15 June 2017, From http://www.linz.govt.nz/sea/tides/sea-level-data/sea-level-data-downloads

Leuzinger, S., Manusch, C., Bugmann, H., & Wolf, A. (2013). A sink-limited growth model improves biomass estimation along boreal and alpine tree lines. *Global Ecology and Biogeography*, *22*, 924–932.

Lockhart, J. A. (1965). An analysis of irreversible plant cell elongation. *Journal of Theoretical Biology*, *8*, 264–275.

Mercado, L. M., Medlyn, B. E., Huntingford, C., Oliver, R. J., Clark, D. B., Sitch, S., … Cox, P. M. (2018). Large sensitivity in land carbon storage due to geographical and temporal variation in the thermal response of photosynthetic capacity. *New Phytologist*, *218*, 1462–1477.

Mielewczik, M., Friedli, M., Kirchgessner, N., & Walter, A. (2013). Diel leaf growth of soybean: A novel method to analyze two-dimensional leaf expansion in high temporal resolution based on a marker tracking approach (Martrack Leaf). *Plant Methods*, *9*, 13.

Minervini, M., Scharr, H., & Tsaftaris, S. A. (2015). Image analysis: The new bottleneck in plant phenotyping. *IEEE Signal Processing Magazine*, *32*, 126–131.

Muller, B., Pantin, F., Genard, M., Turc, O., Freixes, S., Piques, M., & Gibon, Y. (2011). Water deficits uncouple growth from photosynthesis, increase C content, and modify the relationships between C and growth in sink organs. *Journal of Experimental Botany*, *62*, 1715–1729.

Nagelmüller, S., Kirchgessner, N., Yates, S., Hiltpold, M., & Walter, A. (2016). Leaf Length Tracker: A novel approach to analyse leaf elongation close to the thermal limit of growth in the field. *Journal of Experimental Botany*, *67*, 1897–1906.

Nguyen, H. T., Meir, P., Sack, L., Evans, J., Oliveira, R. S., & Ball, M. C. (2017). Leaf water storage increases with salinity and aridity in the mangrove *Avicennia marina*: Integration of leaf structure, osmotic adjustment and access to multiple water sources. *Plant, Cell & Environment*, *40*, 1576–1591.

Nguyen, H. T., Meir, P., Wolfe, J., Mencuccini, M., & Ball, M. C. (2017). Plumbing the depths: Extracellular water storage in specialized leaf structures and its functional expression in a three-domain pressure–volume relationship. *Plant, Cell & Environment*, *40*, 1021–1038.

Ortega, J. K. E. (1985). Augmented growth equation for cell wall expansion. *Plant Physiology*, *79*, 318–320.

Pantin, F., Simonneau, T., & Muller, B. (2012). Coming of leaf age: Control of growth by hydraulics and metabolics during leaf ontogeny. *New Phytologist*, *196*, 349–366.

Pantin, F., Simonneau, T., Rolland, G., Dauzat, M., & Muller, B. (2011). Control of leaf expansion: A developmental switch from metabolics to hydraulics. *Plant Physiology*, *156*, 803–815.

Pfeffer, W. (1903). *The physiology of plants. A treatise upon the metabolism and sources of energy in plants. Volume II. Growth, reproduction, and maintenance* (A.J. Ewart, trans.) (2nd ed.). Oxford: Clarendon Press.

Poire, R., Wiese-Klinkenberg, A., Parent, B., Mielewczik, M., Schurr, U., Tardieu, F., & Walter, A. (2010). Diel time-courses of leaf growth in monocot and dicot species: Endogenous rhythms and temperature effects. *Journal of Experimental Botany*, *61*, 1751–1759.

R Core Team. (2017). *R: A language and environment for statistical computing*. Vienna: Austria.

Rozema, J., Arp, W., Diggelen, J. V., Kok, E., & Letschert, J. (1987). An ecophysiological comparison of measurements of the diurnal rhythm of the leaf elongation and changes of the leaf thickness of salt-resistant dicotyledonae and monocotyledonae. *Journal of Experimental Botany*, *38*, 442–453.

Ruts, T., Matsubara, S., Wiese-Klinkenberg, A., & Walter, A. (2012). Diel patterns of leaf and root growth: Endogenous rhythmicity or environmental response? *Journal of Experimental Botany*, *63*, 3339–3351.

Sadok, W., Naudin, P., Boussuge, B., Muller, B., Welcker, C., & Tardieu, F. (2007). Leaf growth rate per unit thermal time follows QTL-dependent daily patterns in hundreds of maize lines under naturally fluctuating conditions. *Plant, Cell & Environment*, *30*, 135–146.

Schmundt, D., Stitt, M., Jahne, B., & Schurr, U. (1998). Quantitative analysis of the local rates of growth of dicot leaves at a high temporal and spatial resolution, using image sequence analysis. *Plant Journal*, *16*, 505–514.

Steppe, K., De Pauw, D. J. W., Lemeur, R., & Vanrolleghem, P. A. (2006). A mathematical model linking tree sap flow dynamics to daily stem diameter fluctuations and radial stem growth. *Tree Physiology*, *26*, 257–273.

Tran, P., Gritcan, I., Cusens, J., Alfaro, A. C., & Leuzinger, S. (2017). Biomass and nutrient composition of temperate mangroves (*Avicennia marina* var. *australasica*) in New Zealand. *New Zealand Journal of Marine and Freshwater Research*, *51*, 427–442.

Waldron, L. J., Terry, N., & Nemson, J. A. (1985). Diurnal cycles of leaf extension in unsalinized and salinized *Beta vulgaris*. *Plant, Cell & Environment*, *8*, 207–211.

Walter, A., Feil, R., & Schurr, U. (2002). Restriction of nyctinastic movements and application of tensile forces to leaves affects diurnal patterns of expansion growth. *Functional Plant Biology*, *29*, 1247–1258.

Walter, A., Silk, W. K., & Schurr, U. (2009). Environmental effects on spatial and temporal patterns of leaf and root growth. *Annual Review of Plant Biology*, *60*, 279–304.

Zimmermann, D., Reuss, R., Westhoff, M., Geßner, P., Bauer, W., Bamberg, E., … Zimmermann, U. (2008). A novel, non-invasive, online-monitoring, versatile and easy plant-based probe for measuring leaf water status. *Journal of Experimental Botany*, *59*, 3157–3167.

Zweifel, R., Haeni, M., Buchmann, N., & Eugster, W. (2016). Are trees able to grow in periods of stem shrinkage? *New Phytologist*, *211*, 839–849.

SUPPORTING INFORMATION

Additional supporting information may be found online in the Supporting Information section at the end of the article.

How to cite this article: Hilty J, Pook C, Leuzinger S. Water relations determine short time leaf growth patterns in the mangrove *Avicennia marina* (Forssk.) Vierh. *Plant Cell Environ*. 2019;42:527–535. https://doi.org/10.1111/pce.13435